Seismic Detection and Analysis of Underground Laboratory Facilities

Work performed for Institute for Advanced Technology
The University of Texas at Austin

by Bureau of Economic Geology, The University of Texas at Austin
Bob A. Hardage, Principal Investigator
with Michael De Angelo and Randy Remington

Final Report for Year One, contract no. DAAA21-93-C-0101
U.S. Department of the Army
U.S. Army Research Laboratory

May 2001

Seismic Detection and Analysis of Underground Laboratory Facilities

Work performed for
Institute for Advanced Technology
The University of Texas at Austin

by
Bureau of Economic Geology
The University of Texas at Austin
Bob A. Hardage, Principal Investigator
with Michael De Angelo and Randy Remington

Final Report for Year One, Contract no. DAAA21-93-C-0101
U.S. Department of the Army
U.S. Army Research Laboratory
May 2001

Contents

List of Figures

Seismic Detection and Interpretation of Underground Laboratory Facilities

Summary

An abandoned underground tunnel complex at Fort Hood, Texas was made available for project study. The physical size and depth of this tunnel system were similar to the physical dimensions and burial depths of underground laboratory (UGL) targets that are the subject of this UGL Countermeasures program.

The first seismic field test objective at the Fort Hood tunnel system was to determine if cultural activity within a tunnel can be detected with seismic sensors deployed on the surface near an underground facility. The second objective was to try to identify a tunnel target with these same surface-positioned sensors using reflected and refracted seismic wavefields generated by a weight-drop source stationed at locations around the tunnel target.

Seismic test data were recorded with three-component (3-C) geophones to allow vector extrapolation of event arrivals to their subsurface points of origin. The recording system had only 24 active recording channels, which limited the number of 3-D geophones that could be used for target detection and analysis to eight.

Test results verified that cultural activity within a tunnel can be detected by surface-positioned seismic sensors. Point-source disturbances, such as hammering at a fixed location within the tunnel, yielded more interpretable data then did disturbances from a distributed source, such as the movement of air waves along the entire 1000-ft length of the study tunnel when the entry doors were opened and closed. These data show

that passive seismic monitoring of an UGL site will provide valuable information about UGL structure and geometry.

The weight-drop source produced robust seismic illumination of the chosen tunnel target and other near-surface discontinuities in the tunnel area. These data demonstrate that UGL targets can be illuminated appropriately for target analysis purposes with seismic wavefields if an adequate number of moderate-energy source stations are distributed across a target area.

The results shown here are qualitative in nature. Quantitative analysis of the data will be done during the next funding period.

Test Site

The Fort Hood tunnel complex was constructed in the late 1940's as a secure place for weapons storage and assembly. The tunnel system was built to be a self-contained community of chemical laboratories, machine shops, assembly lines, living quarters, and office areas; all sustained by large, internal, diesel-powered electrical generators. The tunnels have not been actively used for the past 15 to 20 years.

A map view of the tunnel complex is shown in Figure 1 superimposed on an aerial photo of the area. The tunnel system is large, as shown by the labeled dimensions. Each major axis of the tunnel is over 1000 feet long. The tunnel passages are large enough for single-lane vehicular traffic. Some rooms along the tunnel are 30 ft high and expand to widths of about 50 ft. The entire tunnel is lined with re-enforced concrete. The thicknesses of the concrete walls, floors, and ceilings are not known. The burial depth of the tunnel is 50 to 100 ft along its course. A section view along the principal axis of the complex is shown in Figure 2.

In summary, the Fort Hood tunnel system has many of the physical characteristics of hostile UGL targets against which countermeasures may have to be taken. The Fort Hood tunnels are an excellent field laboratory for developing geophysical techniques for identifying and analyzing UGL facilities.

Data Acquisition Constraints

There were three constraints on the seismic field tests that were done at Fort Hood: restricted site-access time, adverse weather, and environmental regulations. The restricted-time constraint arose because the tunnel test site was made available to the seismic research team for only one week. Other research obligations further restricted the access time of the team to only two days of that week. The adverse-weather constraint resulted because it rained almost continuously during the two days of field testing. Wet conditions created data transmission problems through the geophone spread cable which resulted in numerous delays to remedy these problems. An environmental constraint was imposed due to the fact that none of the surface vegetation could be damaged by the field operations. A dense ground cover of juniper and small oak trees (Figs. 1, 6, 11, 15) prevented clearing trails for positioning the weight-drop seismic source. All active source stations were located on existing roads and trails, even when these positions were not optimal for target imaging and analysis.

These constraints did not prevent definitive and valuable tests from being done; they simply reduced the number and variety of test conditions that could be investigated.

Seismic Sensors

Three-component (3-C) geophones were used to record seismic test data across the Fort Hood tunnel targets. These types of geophones have three orthogonal sensing coils; one vertical and two horizontal. In conventional oil and gas seismic exploration, these orthogonal motion-sensing elements are called vertical, inline horizontal, and crossline horizontal (Fig. 3). In this UGL work, these three orthogonal geophone responses will be designated as V, H1, and H2, respectively.

The advantage of using 3-C geophones is that they allow the total seismic wavefield, which is comprised of a compressional wave (P-wave) and two shear waves (SV and SH), to be captured. These three principal seismic components (P, SV, and SH) can be identified and distinguished one from the other by their propagation velocities and by their respective particle displacement vectors. The shear modes, SV and SH, travel in shallow strata with velocities that are a factor of 2 to 4 less than the velocity of their companion P wave. The distinctions between the particle motions that they each impart to the Earth as they pass through an observation point are illustrated in Figure 4. These particle displacement vectors cannot be identified if data are recorded with a single-component seismic sensor, such as a hydrophone or a vertical geophone.

A disadvantage of using 3-C geophones rather than convention 1-C vertical geophones is that the number of receiver stations that can be accommodated by a limited-channel recording system is reduced by a factor of 3, because three data channels are required for each receiver station rather than just one data channel.

For the Fort Hood tests, it was decided that it was more important to acquire all components of the seismic wavefield at a few receiver stations so that the basic physics of the illumination process could be analyzed rather than to acquire partial (1-C) wavefield information at a larger number of receiver stations.

Sensor Deployment

The seismic recording system used to acquire these test data could accommodate only 24 data channels which restricted the number of receiver stations to 8. These receivers were deployed across Access Tunnel No. 2 of the Fort Hood complex as shown in Figure 5. The spacing between successive stations was 25 ft (7.6 m). This 8-station spread spanned 200 ft (61 m), which is an adequate array for analyzing reflected wavefields from targets to a depth of 100 ft (30 m). Targets deeper than 100 ft (30 m). can be analyzed used refracted wavefields acquired with this receiver array if adequate source-station offsets are used.

The receivers were deployed beside a gravel road that traversed the area. The higher number (more northern) stations were close (<100 ft [30 m]) to two air shafts that vented diesel engine exhausts from the electrical generation room in the tunnel (Figs. 5 and 6) and to a cooling tower that delivered conditioned air to the tunnel (Fig. 5). These three construction features (ventilation shafts and cooling tower) were selected as observation sites because they should be good conduits by which seismic disturbances within the tunnel would reach the surface.

Cultural Noise Tests

The first objective of this test program was to determine if cultural noise created by work activities within the tunnel would create seismic disturbances that could be detected by geophones placed on the surface. Two types of cultural noise were created: internal hammering and entry-door movement.

Type 1 cultural noise was heavy hammering within the tunnel. A sledge hammer was used to strike the cement floor of the tunnel at sites 1, 2, and 3 shown in Figure 7. Noise site 1 was inside a large electrical generator room that still contained the massive diesel engine that was used to drive the generator. Ventilation shaft B (Fig. 5) was almost directly above this noise site. Noise site 2 was in the tunnel directly outside the generator room and about halfway between ventilation shaft B and the cooling tower (Fig. 5). Noise site 3 was in the largest room of the tunnel, almost directly under the cooling tower. This room was 30 or 40 ft high, of similar width, and 70 to 80 ft long, with large hoists attached to the ceiling. All three of these sites are locations where significant impulsive noise would have occurred when work activity was being done inside the tunnel.

Data generated by these hammer-noise tests are displayed as Figures 8, 9, and 10. The energy source was a sledge hammer swung manually to impact the cement floor at each test site (Fig. 7). The hammer blows occurred at intervals of 1.5 to 2.0 seconds. The surface-based seismic recorder was turned on manually upon receiving a "start" voice command via radio from personnel inside the tunnel. In each test, a 10-s record was acquired.

The data displays (Figs. 8, 9, 10) show the response of the 8-station surface array of 3-C geophones. Three data traces are shown for each receiver station; the vertical geophone response V and the two horizontal geophone responses H1 and H2. A magnified view of the V, H1, H2 responses at receiver station 101 is included in each data plot.

The direct arrivals form the hammer blows exhibit crisp, easily recognizable first breaks on all three geophone channels. These first-arrival events are followed by high-amplitude coda (see insets in Figures 8, 9, 10). A variable number of echo events follow each direct arrival. The number, energy, and periodicity of these echoes depends on the site where the hammer impacts were made, suggesting that local tunnel construction (e.g. room dimensions) control the echo phenomena.

The frequency character of the first-arrival events at receiver station 101 (inset displays, Figs. 8, 9, 10) is similar on the V, H1, and H2 channels. This data behavior implies that the three data components (V, H1, H2) are portions of a single body-wave event that arrives at station 101 at an angle that distributes the wavelet energy among the three orthogonal sensor elements. Consequently, the vector direction along which the wavelet traveled to reach the 3-C receiver can be calculated by hologram analysis. These arrival directions can then be triangulated backward to define a point of origin. The data behavior seen among the V, H1, and H2 data channels in these hammer noise tests is fundamentally different from that observed in the door-noise tests shown later in Figures 12, 13, and 14.

Type 2 cultural noise that was investigated was the seismic disturbances created by opening and shutting the large, metal, entry doors to the tunnel (Fig. 11). The position of the doors in map view relative to the surface sensor array is shown in Figure 7.

The doors were closed sharply and then opened sharply to produce pressure waves in the tunnel complex. The seismic recorder was turned on when a voice "start" command was relayed to the recording engineer from the personnel who opened and shut the doors. Ten-second field records were acquired in each test. Displays of the geophone responses for three tests are shown in Figures 12, 13, and 14.

These data are more complex than data from impulsive, point-source noise generators within the tunnel, such as hammer-generated noise. Impulsive point-source noise generators produced discrete, recognizable direct arrivals and echoes (Figs. 8, 9, 10). In contrast, the air wave moving away from the entry door creates a large, distributed source array along every corridor of the tunnel complex, including tunnel 2 (where the door test was done), as well as tunnels 1 and 3 and their associated connecting tunnels (Fig. 7). Any change in the effective cross sectional area of any tunnel (e.g. doorways to side rooms or entries into large work areas), significant bends and curvatures in the tunnels, and abrupt terminations of any tunnel all become secondary sources of seismic body waves as the channel-guided pressure wave passes these respective features. The result is that the total tunnel complex across its total north-south and east-west extents, acts as a large, distributed source of seismic noise. The resulting data have long, non-ending coda in which it is difficult to recognize distinct arrival events (Figs. 12, 13, 14). These data will be more difficult to interpret than data from impulsive point-source noise generators.

It is interesting to note that the frequency character of door-generated noise on the vertical V sensor differs from the frequency character on the horizontal H1 and H2 sensors (insets, Figs 12 and 14 particularly). The V response is a high-frequency wavelet; the H1 and H2 responses are low-frequency wavelets. This behavior suggests that the data may be a complex mixture of P and S body waves and surface waves. P waves are typically higher frequency data than S waves, implying that the V sensor is capturing P data and the H1 and H2 sensors are recording S data that arrive in a time-overlapped mode with the P data. If true, an additional complication will be introduced into the analysis of these door-noise data.

Active-Source Tests

The second objective of the field test at Fort Hood was to acquire seismic reflection and refraction data across a tunnel target using an active, surface-positioned energy source. The source used in these tests was the Bison EWG-III, a 550-lb (250 kg) accelerated weight-drop unit, that creates a maximum impact of 7000 ft-lbs (9491 joules; 968 kg-m). A zero-time trigger switch could be used when the source was within 100 ft (30 m) of the seismic recorder. This trailer-towed source is shown in Figure 15. A close-up view of the source baseplate and of the accelerometer deployed on the baseplate to detect time-zero of the impact is included as Figure 16.

The weight-drop source was deployed at the station positions defined in Figure 17. The distance between adjacent source stations was 25 ft (7.6 m), the same interval that was used for the receiver stations. Source stations began at receiver station 101 and extended twelve stations beyond receiver station 108, ending at source station 120. At receiver station 105 where there were small openings in the timber cover, off-line source stations were extended three station intervals east and west of the 20-station 2-D profile.

Representative responses recorded by the surface receiver spread are shown as Figures 18, 19, 20, and 21. A response to an impulse located within the receiver spread is shown in Figure 18; off-end source responses are illustrated in Figure 19 and 20; and an off-line source response is included as Figure 21. The cable connecting the time-zero baseplate accelerometer (Fig. 16) to the seismic recorder would not extend to the farthest off-end source stations. The recorder was started by a verbal radio command from these stations, causing the field records to have variable time-zero origins as in Figure 20. This floating time-zero should not present insurmountable data-processing difficulties.

It is difficult to see reflection and refraction events from the tunnel target in the data displays because these display formats show the total 3-C response and do not segregate the data into their V, H1, and H2 responses. These wavefield separations will be done in the subsequent project funding period. The key points to emphasize regarding these data are that they are robust, have good signal-to-noise character, and definitely illuminated the tunnel target. The challenge now is to extract target-specific information from the data.

Conclusions

Good quality 3-component seismic test data were acquired across the tunnel target studied at Fort Hood. Passive noise tests provided one immediate answer, that being that impulsive, point-source noise generators that produce minimal pressure waves that traverse the length of the tunnel are optimal noise sources for target detection and analysis. Any noise generator that produces a robust air wave that propagates the entire length of the tunnel results in a guided channel wave that creates multiple secondary sources throughout the total tunnel complex. The myriad of distributed sources created by this guided wave results in a composite seismic wavefield that is difficult to analyze and interpret.

The test data are expected to demonstrate that any seismic data acquired to evaluate UGL facilities should be recorded with 3-component geophones rather than with single-component geophones. The reason is that the 3-C response at each receiver station can be analyzed to indicate the vector direction along which an event travels to that station. These arrival vectors can then be extrapolated back to their points of origin to identify target coordinates. Such vector analyses cannot be done with single-component seismic sensors. Vector-based analysis of these test data will be a key focus of the next study phase.

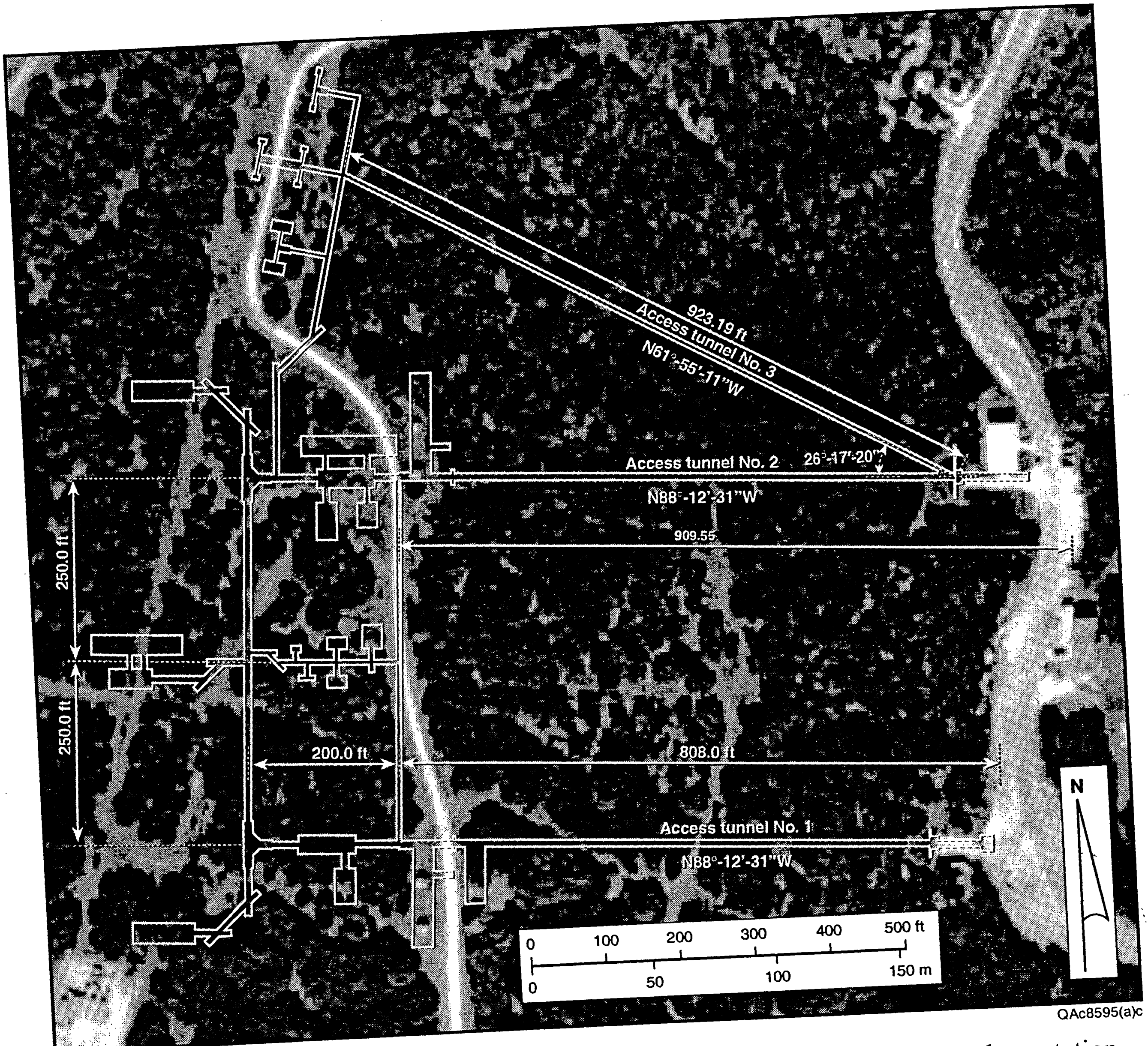

Fig. 1. Fort Hood tunnel system imposed on aerial photograph of surface roads and vegetation.

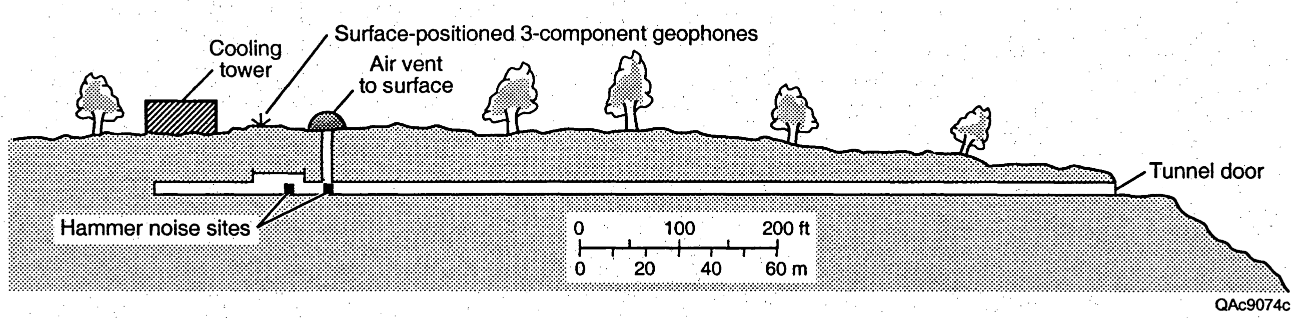

Fig. 2. Generalized section view of Fort Hood tunnel system along profile of Access Tunnel No. 2 (Fig. 1).

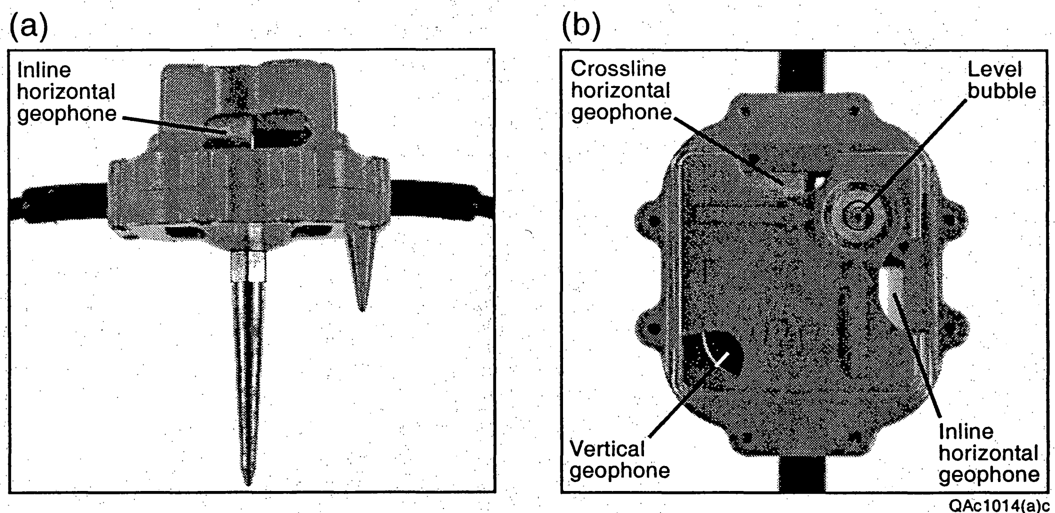

Fig. 3. Cutaway views of 3-component geophone (a) Side view. (b) Vertical view.

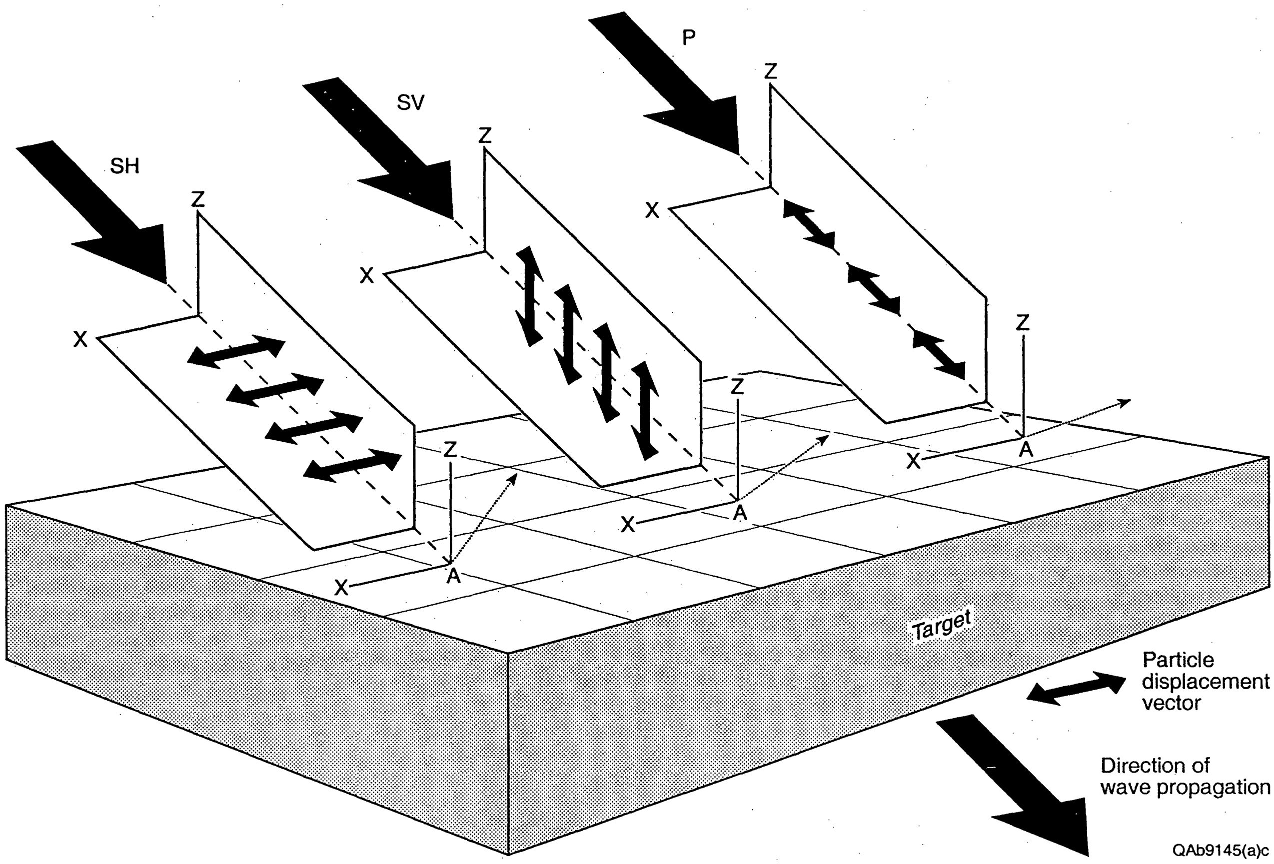

Fig. 4. Distinction between the three illuminating wavefields created by a seismic source. P is a compressional wave that causes rock particles to oscillate in the direction that the wavefront is propagating. SV and SH are shear waves that cause rock particles to oscillate perpendicular to the direction that the wavefront is moving.

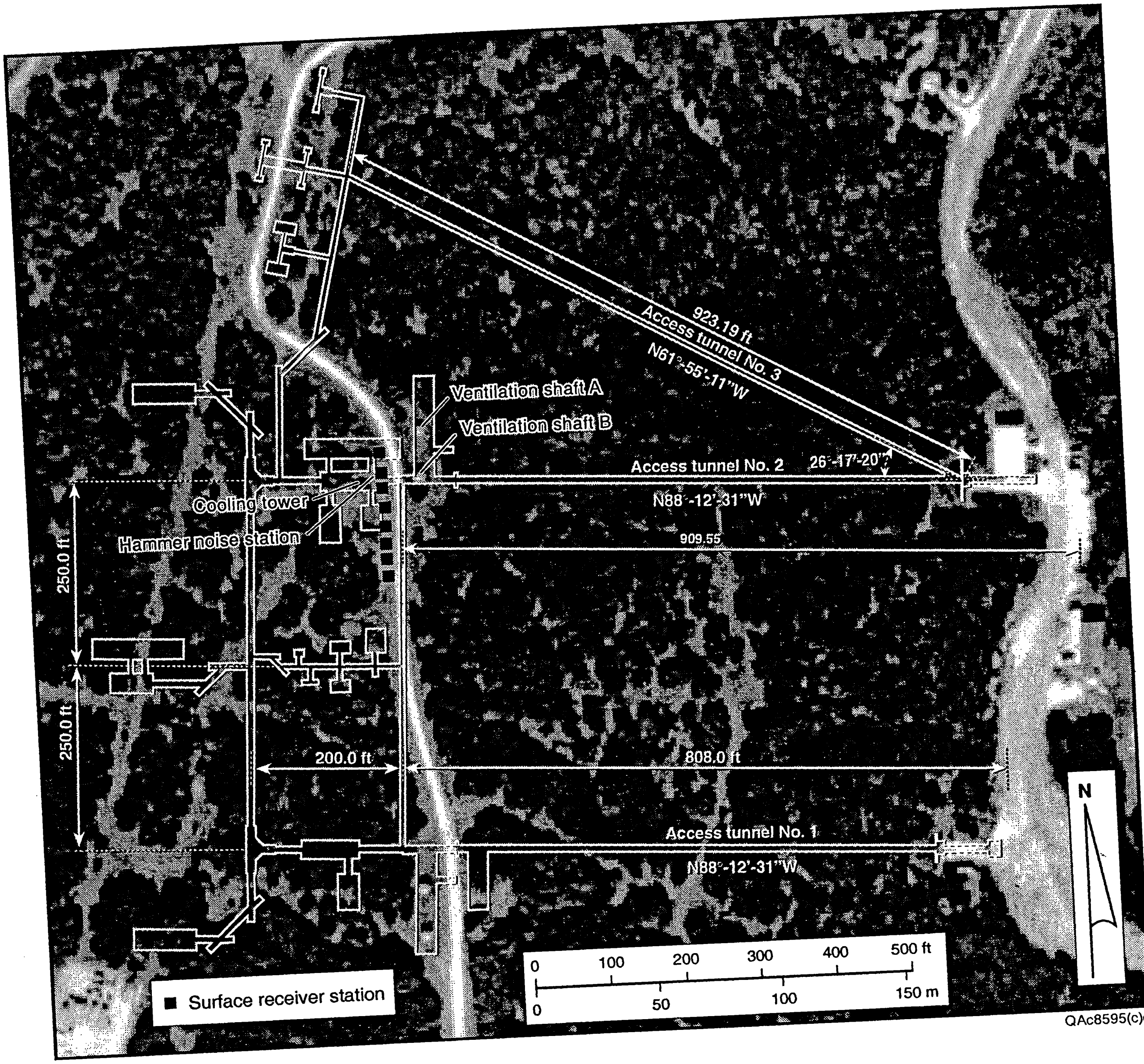

Fig. 5. Deployment of surface seismic sensors across the tunnel target.

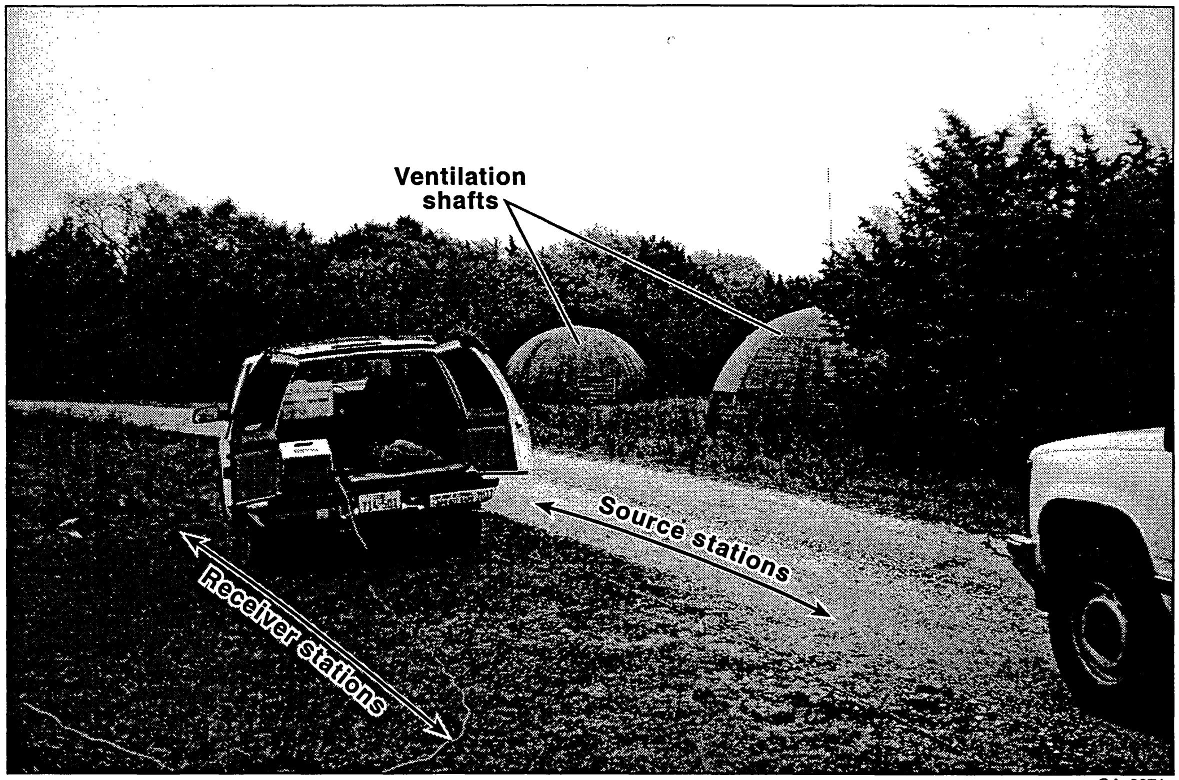

Fig. 6. Surface view of receiver array area near the ventilation shafts shown in Figure 5.

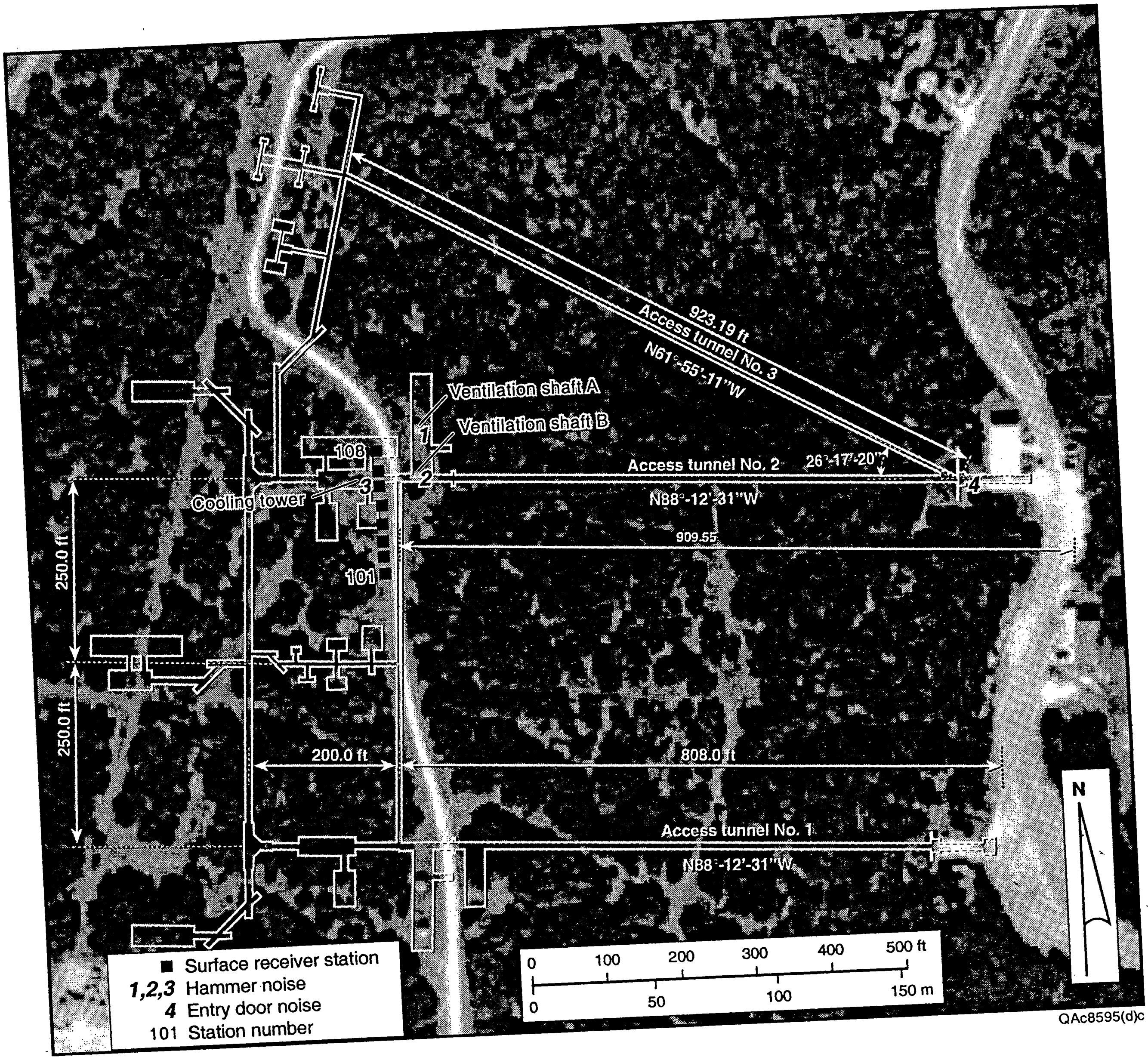

Fig. 7. Locations of cultural noise sites created inside the test tunnel.

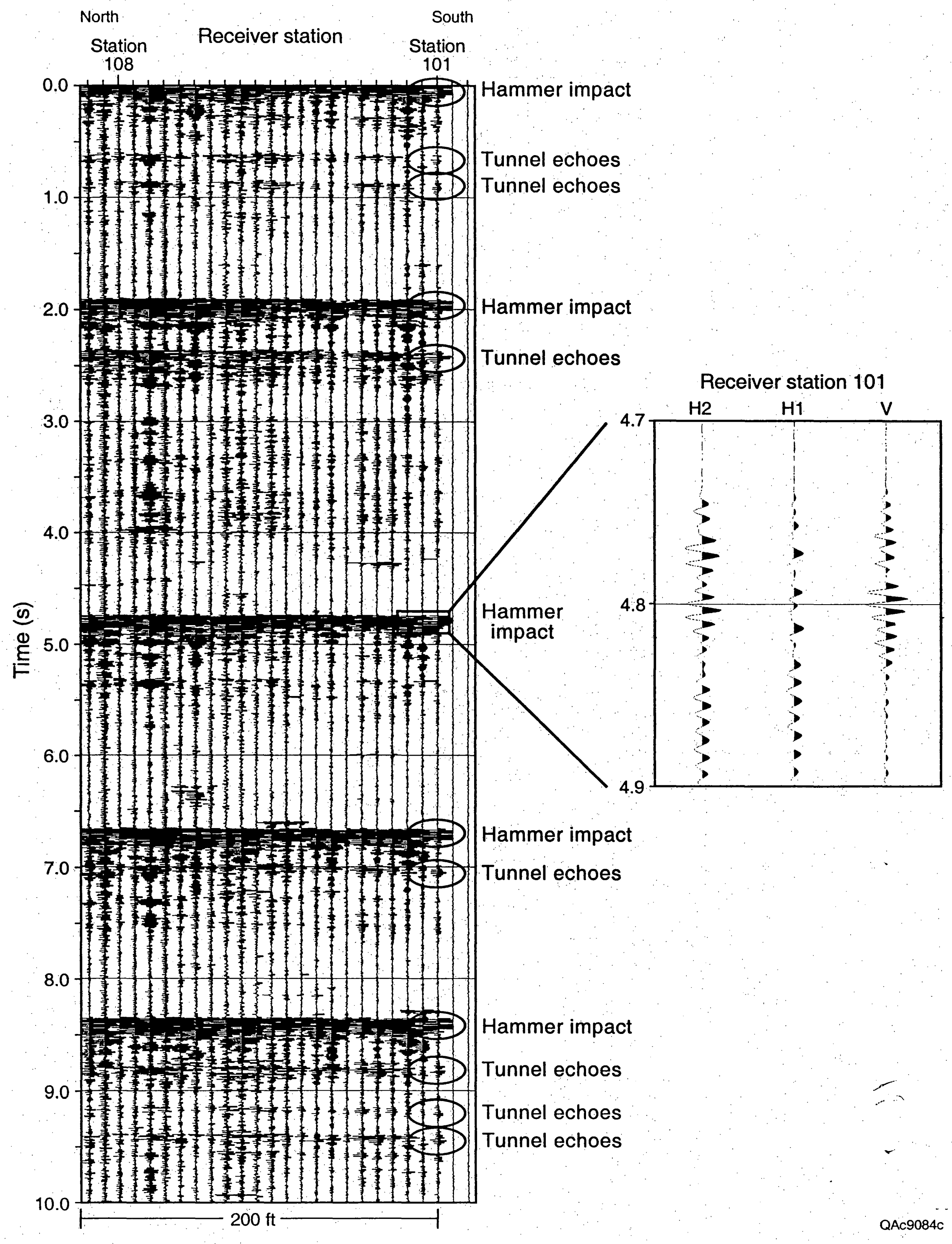

Fig. 8. Data recorded by 3-C surface geophones when hammer noise was created at site 1 in tunnel (Fig. 7).

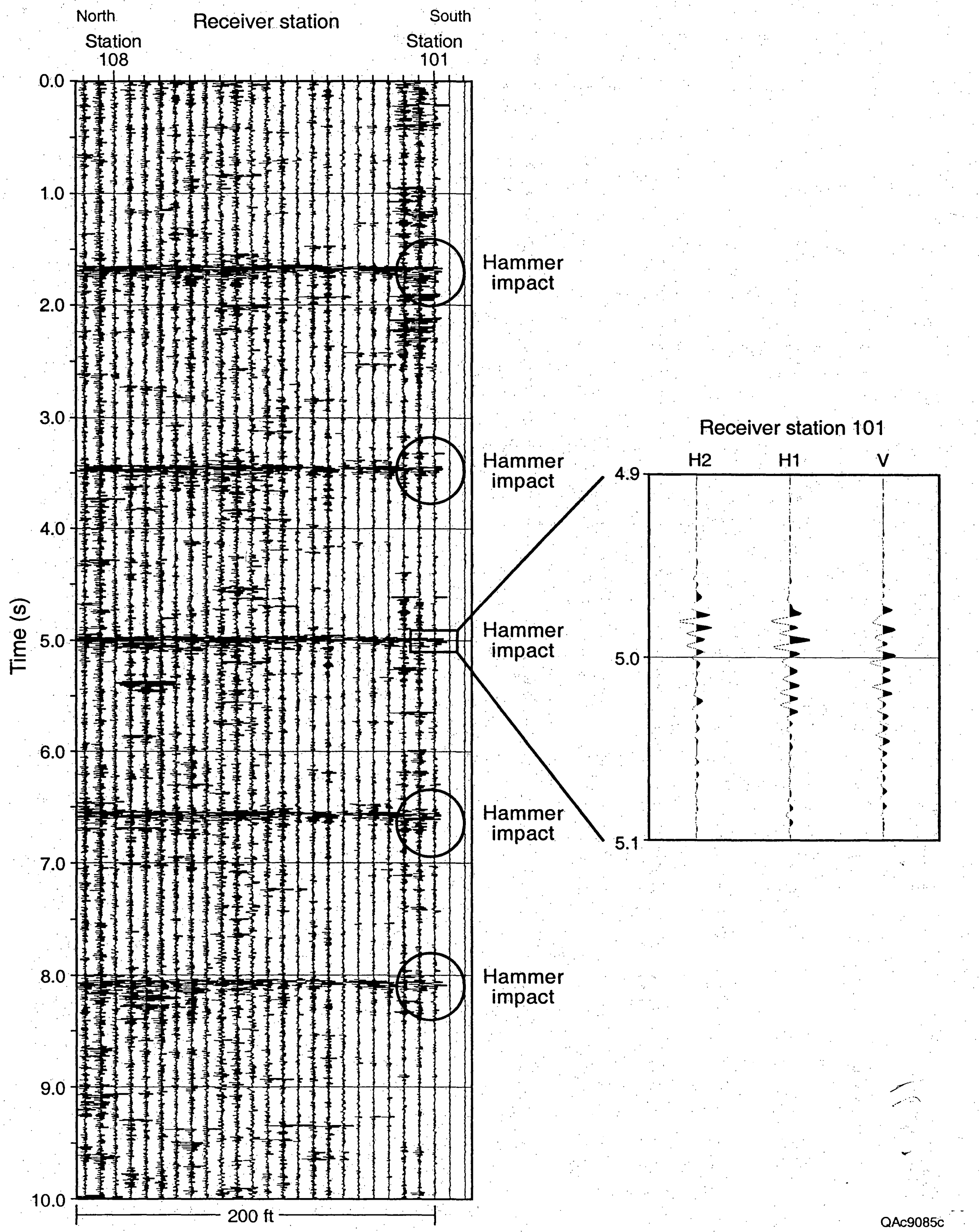

Fig. 9. Data recorded by 3-C surface geophones when hammer noise was created at site 2 in tunnel (Fig. 7).

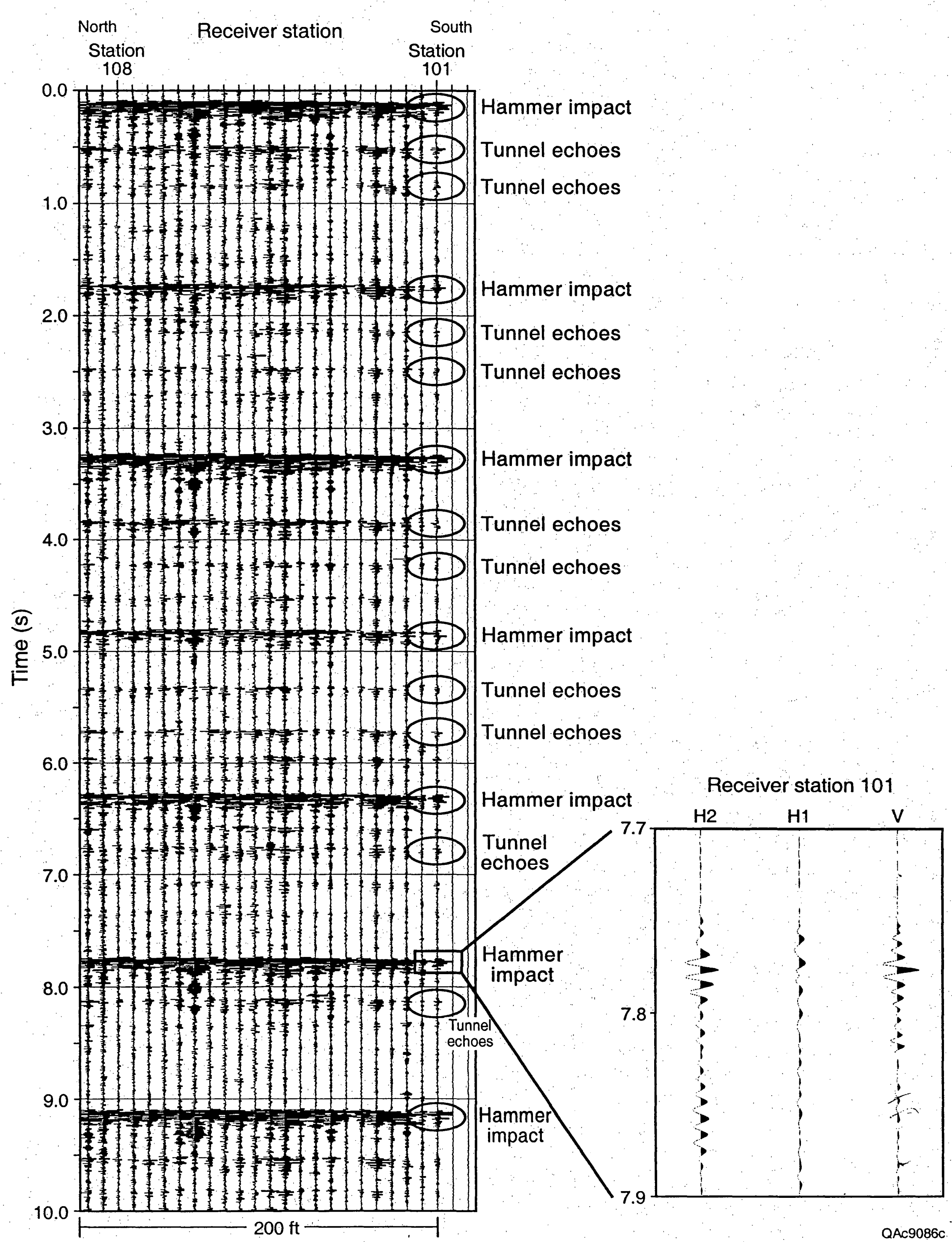

Fig. 10. Data recorded by 3-C surface geophones when hammer noise was created at site 3 in tunnel (Fig. 7).

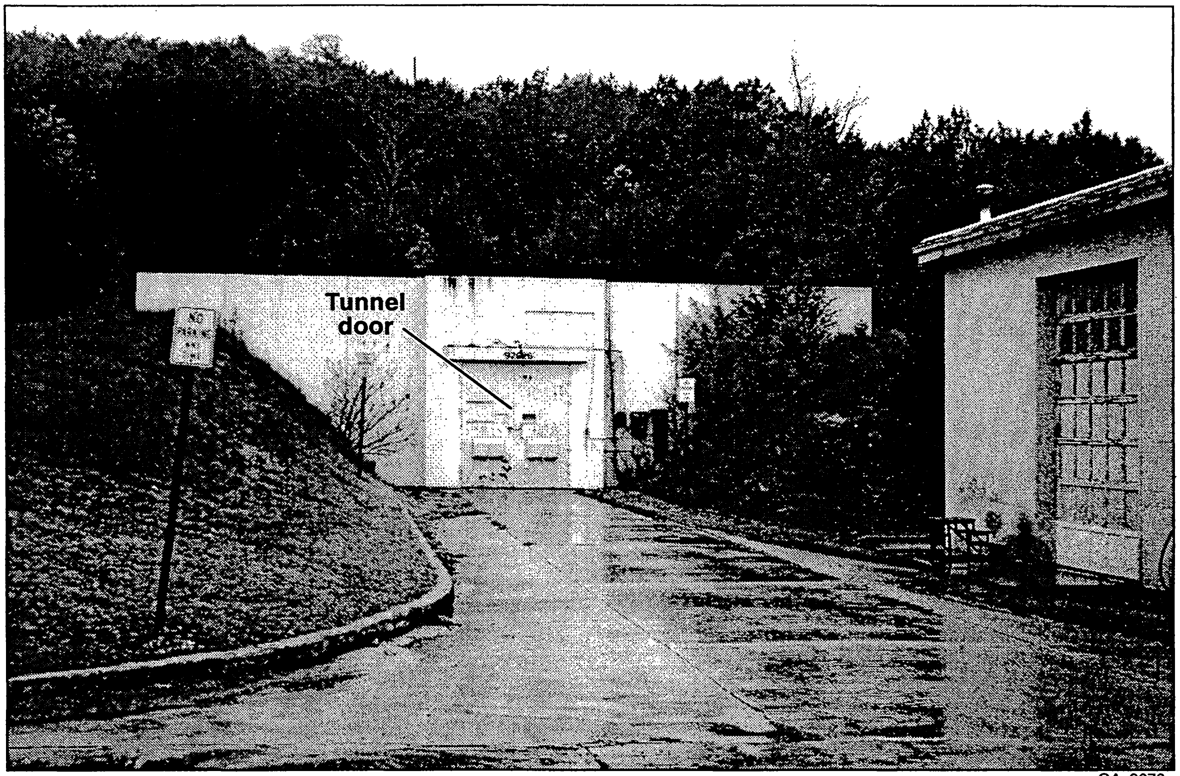

QAc9070c

Fig. 11. Entry to tunnel. The metal doors are massive, being ~12 ft (3.7 m) wide and 16 ft (4.9 m) high.

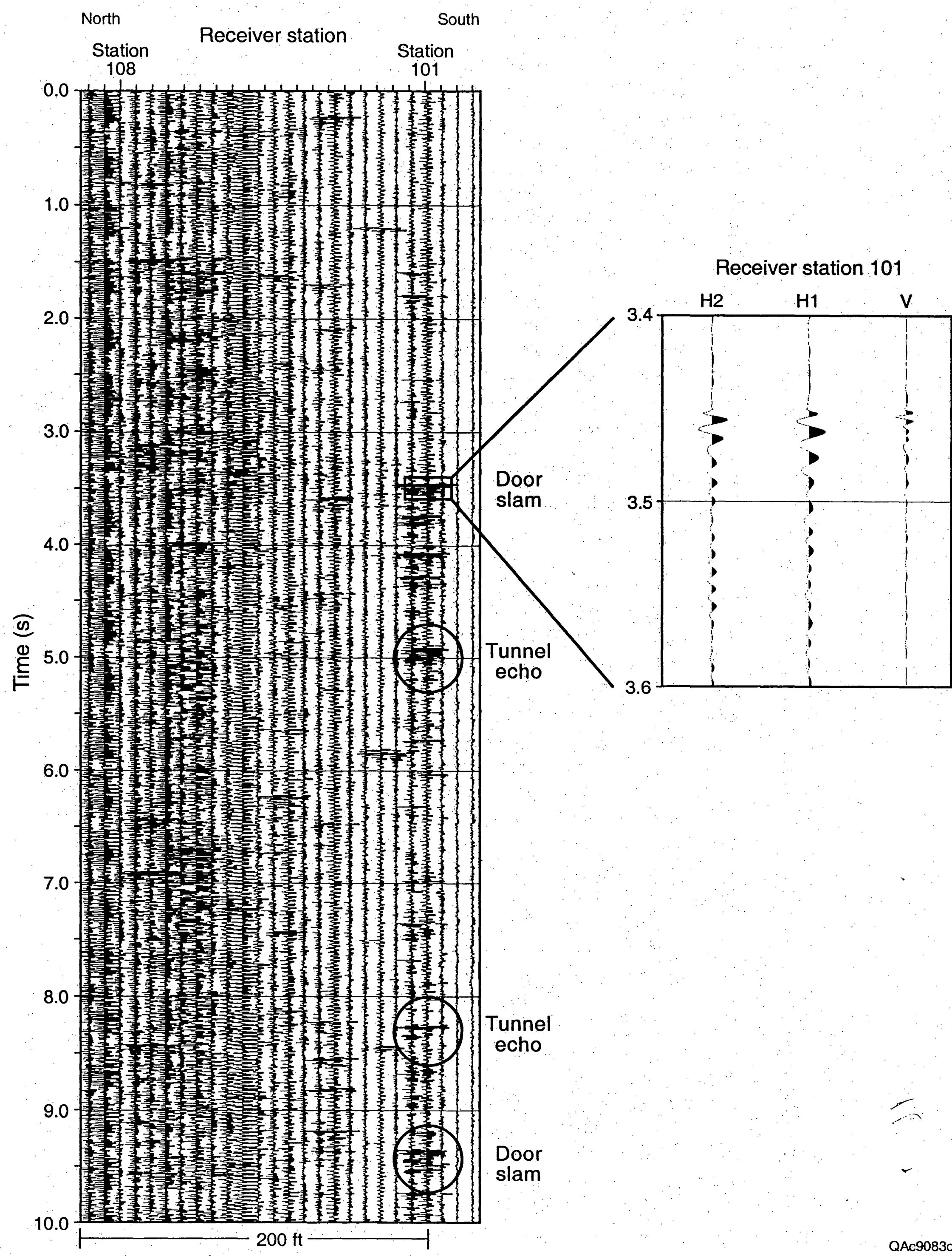

Fig. 12. Data recorded by 3-C surface geophones when tunnel door was opened and closed (Test 1).

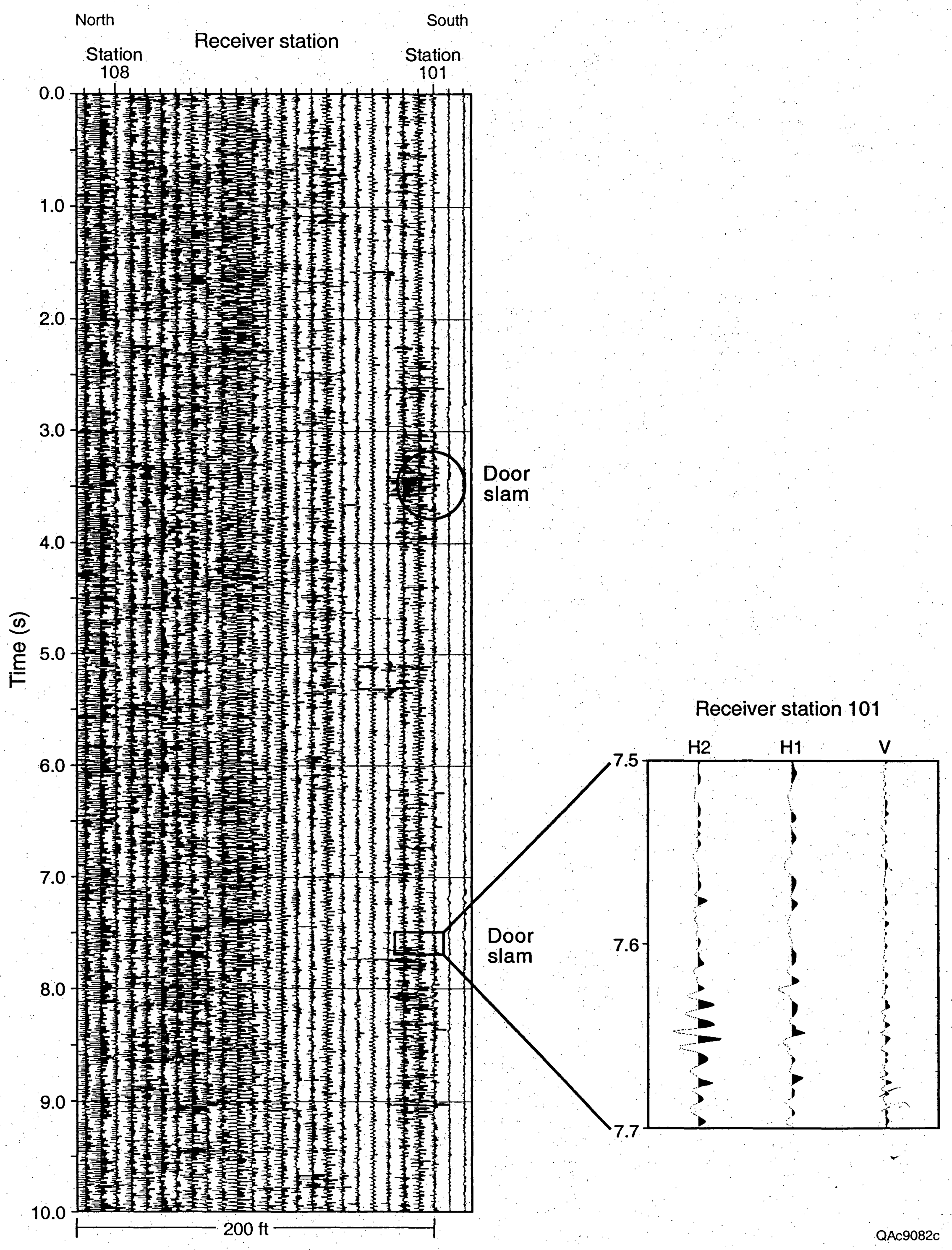

Fig. 13. Data recorded by 3-C surface geophones when tunnel door was opened and closed (Test 2).

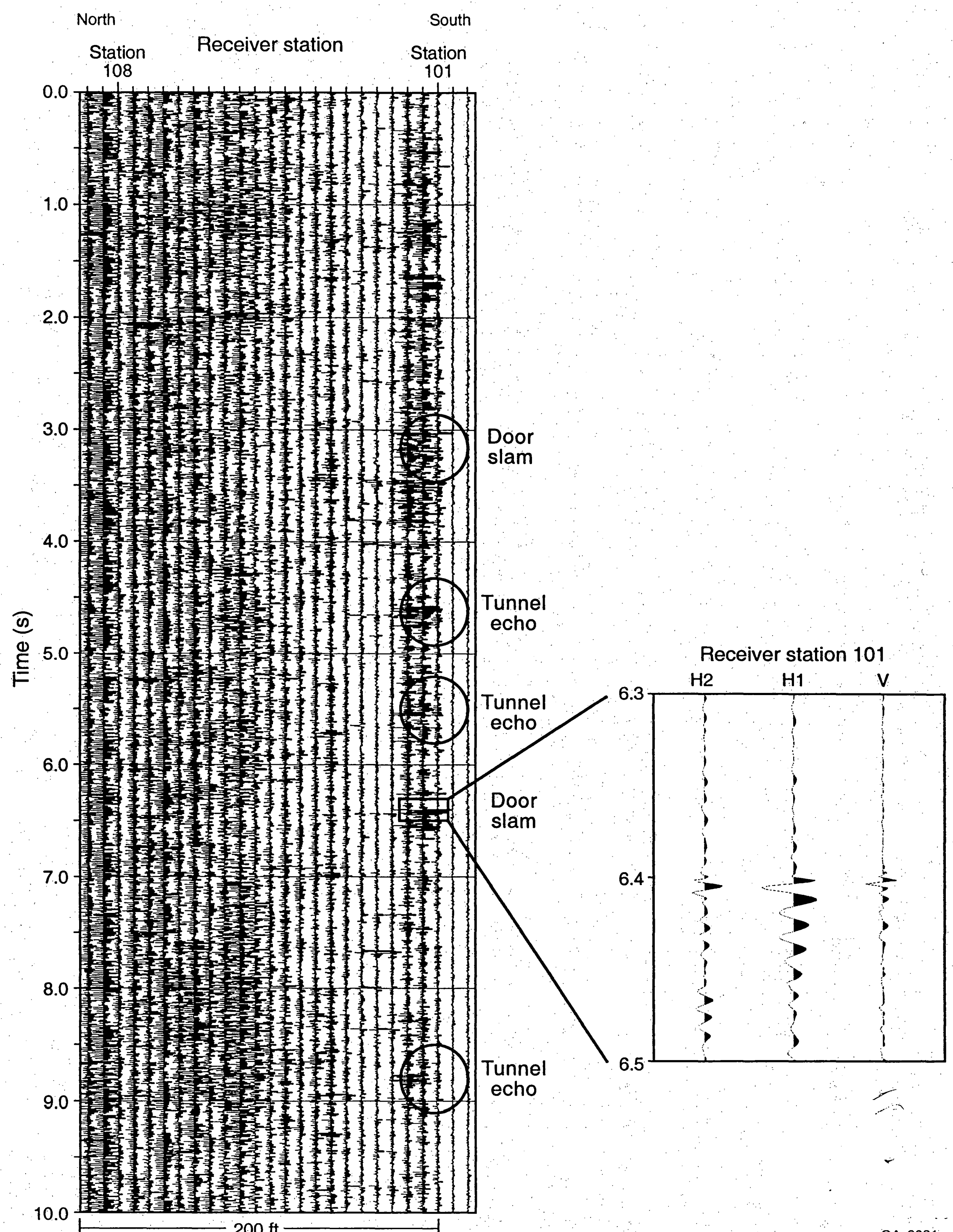

Fig. 14. Data recorded by 3-C surface geophones when tunnel door was opened and closed (Test 3).

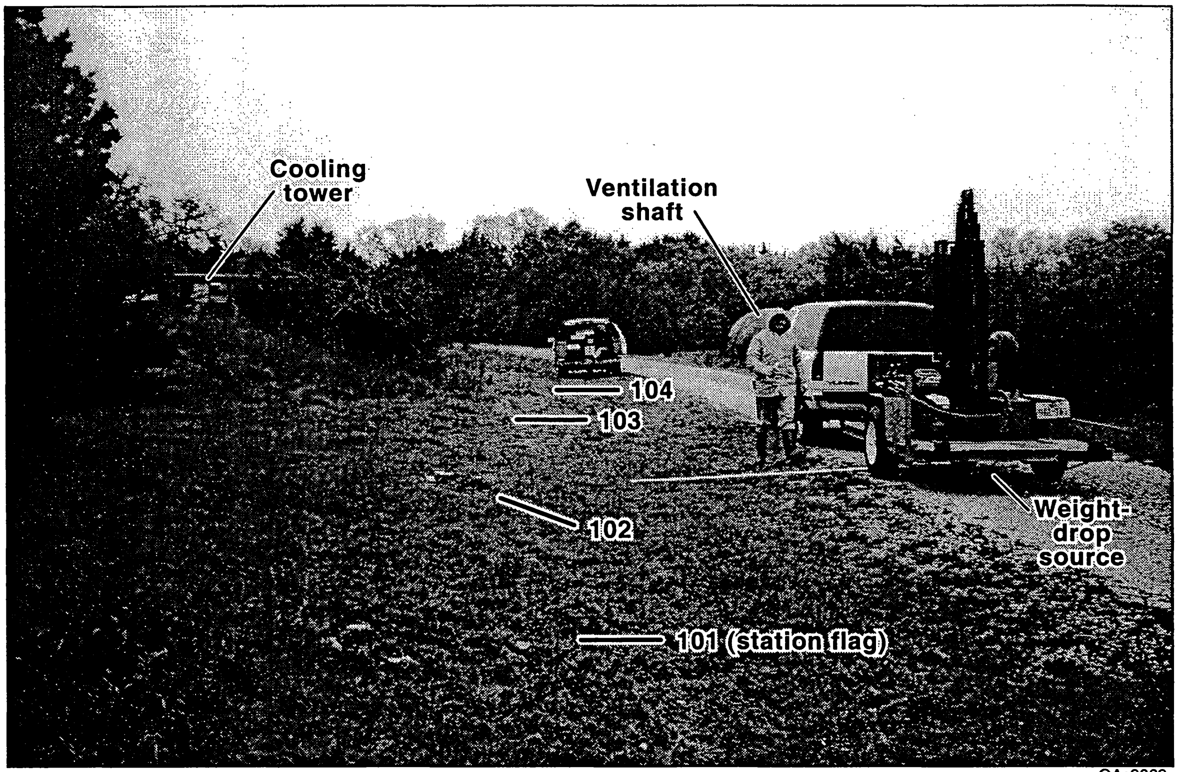

Fig. 15. Vertical weight-drop source being deployed across the tunnel target.

Fig. 16. Baseplate of weight-drop source and accelerometer used to establish time zero of the seismic impulse.

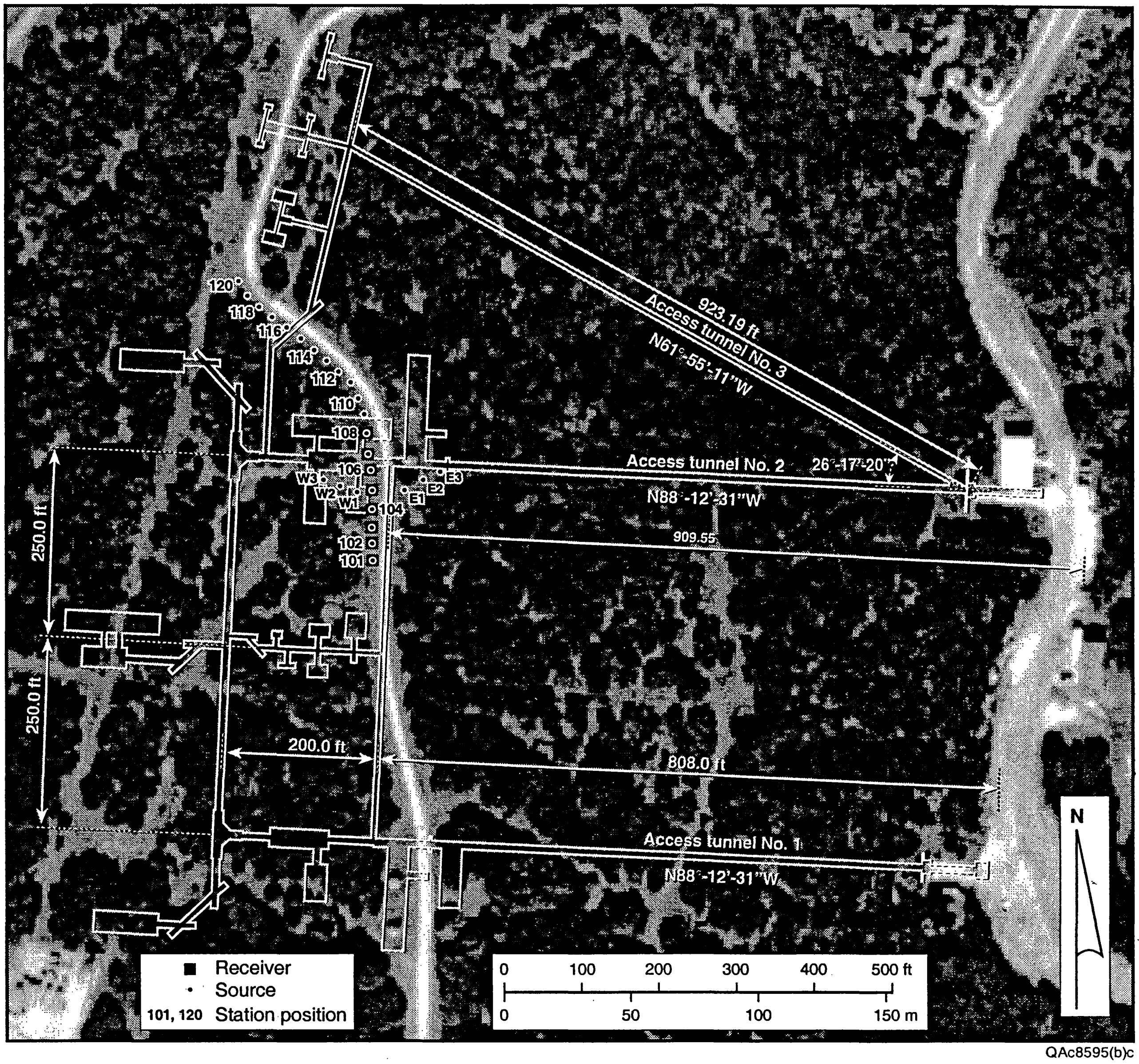

Fig. 17. Map view of source stations across target area.

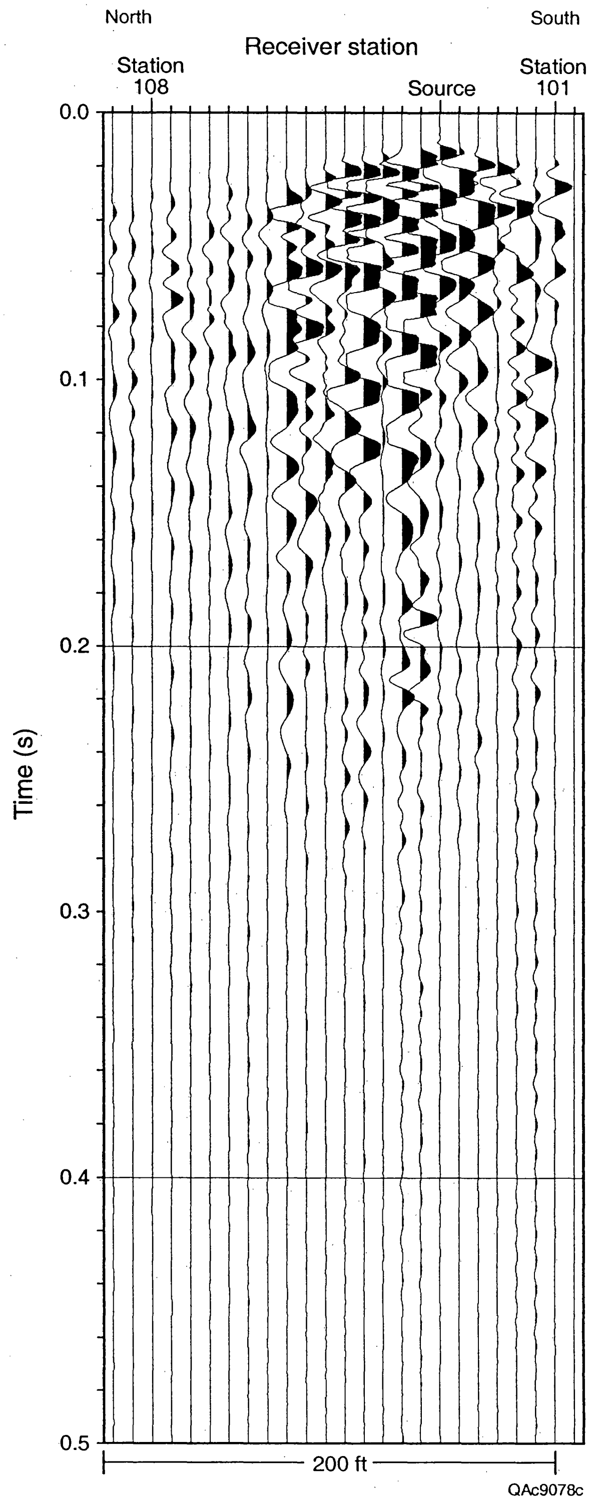

Fig. 18. Data recorded by 3-C surface geophones when weight-drop source was impulsed at source station 103.

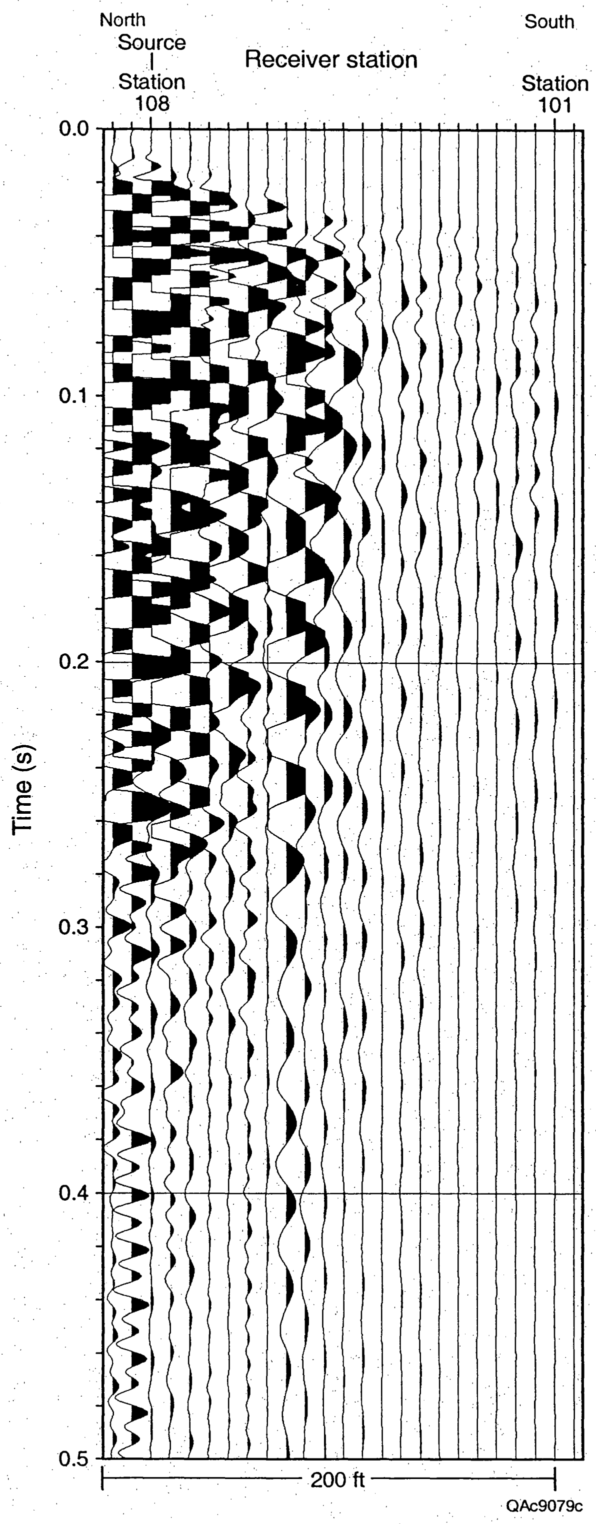

Fig. 19. Data recorded by 3-C surface geophones when weight-drop source was impulsed at source station 108.

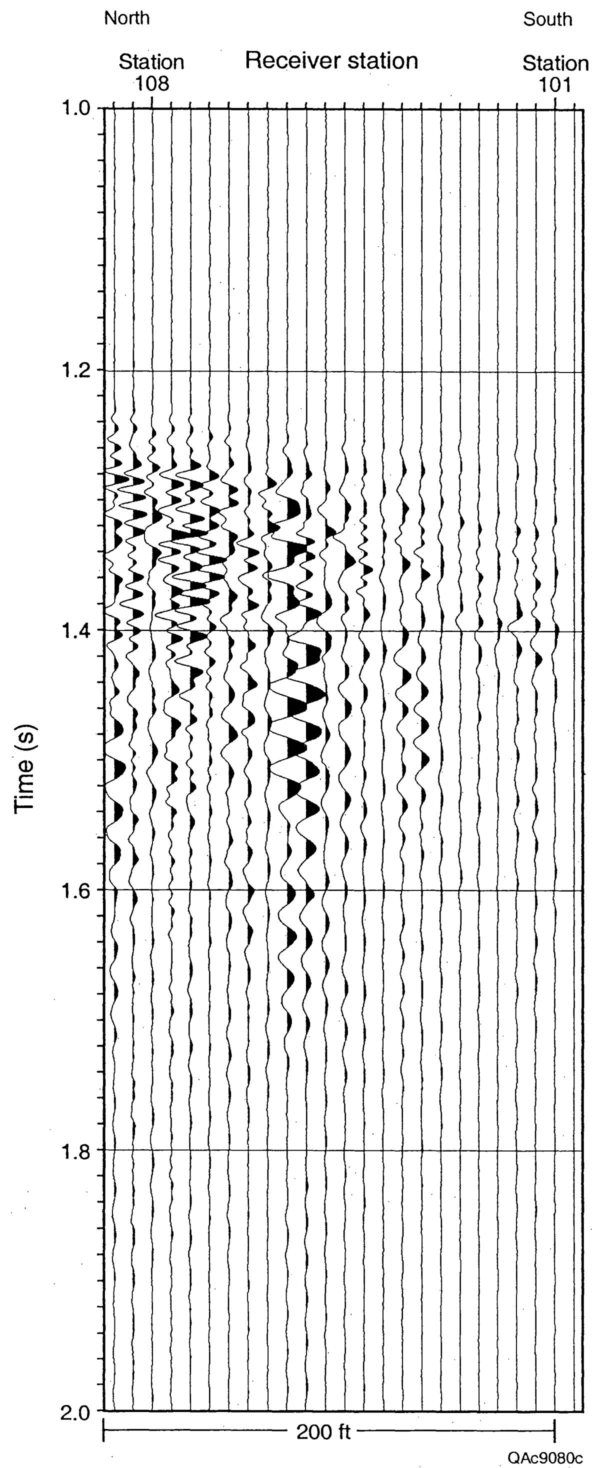

Fig. 20. Data recorded by 3-C surface geophones when weight-drop source was impulsed at off-end source station 120.

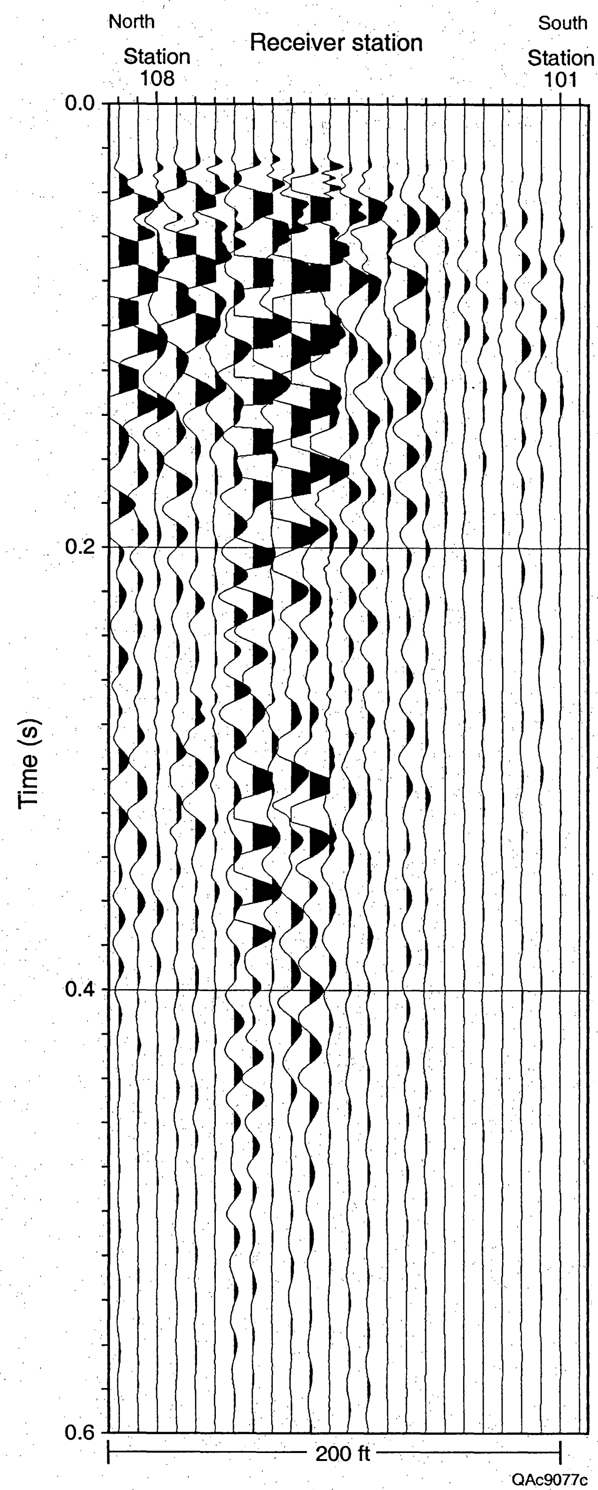

Fig. 21. Data recorded by 3-C surface geophones when weight-drop source was impulsed at off-line source station W2.